Original Article

Corresponding Author:

Hanlin Li, Loughborough Design School, Loughborough University, Loughborough, UK, LE11 3TU

Simulations of engine knock flow field and wave induced fatigue of a downsized gasoline engine

Wang Wenrui[1], Lu Yu[1], Li Zhiyong[2], Hanlin Li[3]

1 School of Mechanical Engineering, University of Science and Technology Beijing, Beijing 100083, China

2 Beijing Institute of Strength and Environment, Beijing 100083, China

3 Loughborough Design School, Loughborough University, Loughborough LE11 3TU, UK

Abstract:

A mathematical correlation is developed, based on the thermodynamic model of a downsized gasoline engine, to establish the numerical relationship among the thermodynamic parameters of the combustion chamber. In the developed numerical model, the in-cylinder pressure curves of various operation condition are simulated by varying the air-fuel ratio in the cylinder, and the associated knock characteristics are recorded. The accuracy of the numerical simulation results is verified against the knock excitation experiment. Then, based on the Rover K16 gasoline engine, a simulation model is developed to simulate the engine knock in the combustion chamber and observe the force acting on the top surface of the piston. The results show that the forces act on the piston top surface are varying at various locations at the same time, and the largest forces occur at the edge of the piston and followed by the piston centre. Then, by comparing the thermo-mechanical coupling strength of the piston under different operating conditions, the results show that the occurrence of the knocking does not exceed the piston's strength limit. However, the stress and deformation value of the piston is increased significantly, and the failure point of the piston position is changed. Finally, based on the calibrated strength results, the piston durability is predicted for various engine knock conditions. The results show that the initial damage of piston in the process of detonation at the surface of the piston pin hole and the joint of the piston cavity. The gasoline engine finally has a predicted mileage of 253,440 km continuously which meet the prescribed mileage of 220,000 km.

Keywords:

Downsized gasoline engine, Combustion chamber, Detonation wave, Strength, Fatigue

1 Introduction

With the application of extreme downsizing technology, the instability of the combustion process of the gasoline engine and detonation tendency is increased. Hence, the fuel economy is reduced, and the gasoline engine components are severely damaged. Especially, the piston is working in a harsh condition that involves high speed, high pressure and high temperature, and therefore, the piston must have sufficient strength [1]. At present, super detonation has become the biggest obstacle for gasoline engines to continue to improve power density and reduce fuel consumption. Many automotive engine manufacturers, fuel and lubricant companies and related research institutes at home and abroad are studying the mechanism and suppression strategy of super detonation [2,3]. Under this circumstance, the study of the engine knock characteristics and piston strength calibration has both theoretical and engineering values in terms of the research for safety and reliability of the downsized engine [4].

Currently, the research on knocking characteristics is mainly through the method of simulation and experiment and focused on the flow field law in the combustion chamber during the knocking phenomena. The main research direction of the piston strength is thermo-mechanical coupling strength verification in natural aspiration engine [5]. Therefore, this is a lack of studies on the impact of cylinder pressure excitation effect on the piston stress distribution and strength in a downsized engine during the knock occurrence [6]. Compared with the existing research, the novelty of this paper is to simulate the strength and life of the engine piston after bearing multiple high-frequency knock shocks, instead of studying the mechanism of knocking and how to suppress knocking. Nobody has studied it yet.

Traditional engine development sector believes that there is a relationship amongst various engine components with respect to their durability. Though the analogue design concept, using the pistons, piston cylinders or cranks as research objects, the strength of each engine component can be obtained. The selected object of this study is a small-enhanced engine piston component, and the primary research interest is focused on the strength calibration and durability analysis of the piston structure under continuous high-frequency detonation. In this paper, we established the numerical correlation between the thermodynamic parameters of the combustion chamber based on a downsized gasoline engine thermodynamic system [7]. By changing the Air-Fuel Ratio (AFR) in the cylinder, the in-cylinder pressure curves under naturally aspirated, supercharged and knocking are obtained. The accuracy of the numerical simulation results is verified against the knock excitation experiment [8]. Based on the Rover K16 gasoline engine model, a simulation model is developed to simulate the knocking phenomenon in the combustion chamber, and the knock pressure excitation is applied to the top of the piston. The developed model is used to observe the stress and deformation of the piston under thermo-mechanical coupling effect in different operation conditions and verify the thermos-mechanical coupling results under the engine knock in terms of the strength and clearance requirement.

Based on the strength calibration results, the durability of the piston under the knocking condition is predicted.

Using the research method of this paper, the fatigue damage of gasoline engine components in the detonation environment can be studied, and then the combustion chamber components can be improved, according to the detonation damage mechanism and the damage influence force, until the gasoline engine performance and durability index are reached. There is an important theoretical and practical significance for the reliable operation of downsized engines without inhibiting the occurrence of knocking.

2 Engine Knock Modelling

2.1 Thermodynamic model of a downsized gasoline engine

Fig. 2-1 is a schematic diagram that shown the simplified thermodynamic model of the combustion chamber, which consists of the top surface of the piston, the cylinder wall and the bottom surface of the cylinder head that valves are placed. The state of the working fluid in the cylinder is expressed by three basic parameters: pressure (p), temperature (T) and mass of the working fluid (m). The entire operation process is represented using the equation of state for an ideal gas (Eq. 2-1), the mass conservation equation (Eq. 2-2) and the energy conservation equation (Eq. 2-3 & 2-4), as the following:

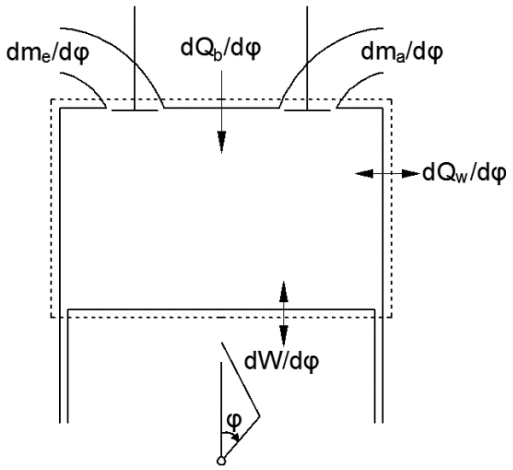

Figure2-1: Schematic diagram for the thermodynamic model of the combustion chamber

Equation of state for ideal gas:

$$pV = mRT \tag{Eq. 2-1}$$

Mass conservation equation:

$$\frac{dm}{d\varphi} = \frac{dm_b}{d\varphi} + \frac{dm_e}{d\varphi} + \frac{dm_a}{d\varphi} \tag{Eq. 2-2}$$

Energy conservation equation:

$$\frac{d(mu)}{d\varphi}=\frac{dQ_b}{d\varphi}+\frac{dm_e}{d\varphi}h_2-\frac{dm_a}{d\varphi}h-\frac{dQ_w}{d\varphi}-p\frac{dV}{d\varphi} \quad \text{(Eq. 2-3)}$$

$$\frac{du}{d\varphi}=\frac{\partial u}{\partial T}\frac{dT}{d\varphi}+\frac{\partial u}{\partial \alpha_m}\frac{d\alpha_m}{d\varphi}=C_v\frac{dT}{d\varphi}+\frac{\partial u}{\partial \alpha_m}\frac{d\alpha_m}{d\varphi} \quad \text{(Eq. 2-4)}$$

where, p—in-cylinder gas pressure, MPa

V—cylinder volume, m^3

m—mass of in-cylinder gas, kg

R—gas constant, J/(mol·K)

T—in-cylinder gas temperature, K

m_b—mass of burned gas, kg

m_e—mass of air flow into the cylinder, kg

m_a—mass of exhaust gas, kg

Q_b—combustion heat release, kJ

Q_w—heat transferred through the walls, kJ

h—enthalpy of the working gas, kJ/ kg

h_2—Specific enthalpy of intake valve, kJ/ kg

C_v—specific heat at constant volume, kJ/(kg/K)

α_m—instantaneous excess air ratio,

The temperature changes of the working fluid inside the cylinder can then derived by combining Eq. 2-2, Eq. 2-3 and Eq. 2-4 together, and be expressed as:

$$\frac{dT}{d\varphi}=\frac{1}{mC_v}\left(\frac{dQ_b}{d\varphi}+\frac{dm_e}{d\varphi}h_2-\frac{dm_a}{d\varphi}h-\frac{dQ_w}{d\varphi}-p\frac{dV}{d\varphi}-u\frac{dm}{d\varphi}-m\frac{\partial u}{\partial \alpha_m}\frac{d\alpha_m}{d\varphi}\right) \quad \text{(Eq. 2-5)}$$

The in-cylinder pressure is determined by combining Eq. 2-1 and the ideal gas equation (Eq. 2-1).

2.2 Boosting simulation and knocking characteristic analysis

The fundamental principle of boosting technology is to force more air into the combustion chamber through various pressurization method, and thus, more fuel can

be burned per working cycle [9]. As a result, the combustion in the cylinder is more intense, and the higher average effective pressure leads to an increase in the engine power output. The mean effective pressure (Pm) is the effective work emitted by the working volume per cylinder of the gasoline engine working cycle. The higher the Pm value, the more work is output from the unit cylinder working volume, and hence, the better the engine's power.

From equation Eq. 2-6 below, it can be seen that the most effective way to increase the pressure is to increase the intake air density ρ_s

$$P_{\mathrm{m}} = \frac{H_u}{L}\rho_s\varphi_c\eta_m\eta_t \quad \text{(Eq. 2-6)}$$

Where, L = The amount of air actually supplied per kg of fuel

ρ_s = intake air density, kg/m3

φ_c = Aeration coefficient

η_m = Mechanical efficiency

η_t = Indicating thermal efficiency

The principle of the gasoline engine boosting technology is to increase the intake air density to increase the amount of air entering the cylinder. Therefore, more fuel can be burned per cycle, so that the mean effective pressure is improved, and a larger engine output power is obtained. In general, the boosted power can be increased by 40%-60% or more than the original.

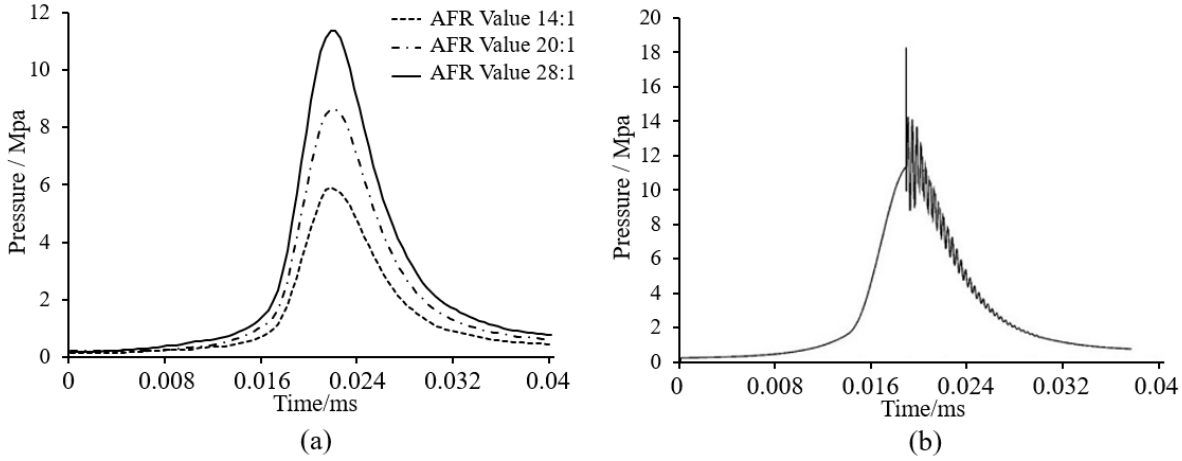

Figure2-2: Cylinder Pressure curves under various conditions

The gasoline engine boosting effect is simulated by changing the air-fuel ratio inside the cylinder. In this paper, AFR is set to 14:1, 20:1 and 28:1 to generate low, medium and high in-cylinder pressure respectively. By applying Eq. 2-5, the in-

cylinder pressure under these three conditions is determined and shown in Fig. 2-2(a). The maximum cylinder pressure for AFR of 14:1, 20:1 and 28:1 is 6MPa, 9MPa and 12 MPa, respectively. As the engine is further downsizing, the probability of the knock occurrence is also increased. According to the typical literature of the existing literature [10,11], the cylinder pressure oscillation curve under knocking is obtained by applying the vibration attenuation function to the pressure curve that determined by Eq. 2-5 previously. Fig. 2-2(b) indicates the in-cylinder knock pressure while AFR is 28:1. As shown in Fig. 2-2(b), the in-cylinder knocking pressure suffered a huge oscillation with an amplitude of nearly 10MPa when the knock occurred initially and followed by a pressure fluctuation of gradually attenuating amplitude with an oscillation frequency of up to 10 kHz, and finally, this pressure is becoming steady. The impact of this knocking occurrence on the combustion chamber components fatigue is obvious [12].

3 Knocking Experiment and Validation

3.1 Method of Knocking Excitation Experiment

A high-temperature capacitive pressure sensor is used to detect the knocking excitation signal. The working principle of this sensor is that the pressure wave in the cylinder is directly sensed by the sensor diaphragm, a slight displacement is then formed between the diaphragm and the medium, and this displacement is increasing with an increase in the detected pressure, and finally, the resistance of the sensor is changing accordingly. The structure of this high-temperature capacitive pressure sensor is shown as Fig. 3-1 below. The electronic circuit is implemented to detect this change in resistance and generate an output signal corresponding to the pressure of the knocking. The sensor is attached to the top of the cylinder along with a charge amplifier connected in order to strengthen the signal, as the original output signal from the piezoelectric crystal is very weak. The amplified output signal is then passed through a rotary encoder, and then the in-cylinder pressure curve is captured for the duration of 50 cycles, and the final signal generated from the 50 cycles is the knock excitation signal. Fig. 3-2 indicates this entire process.

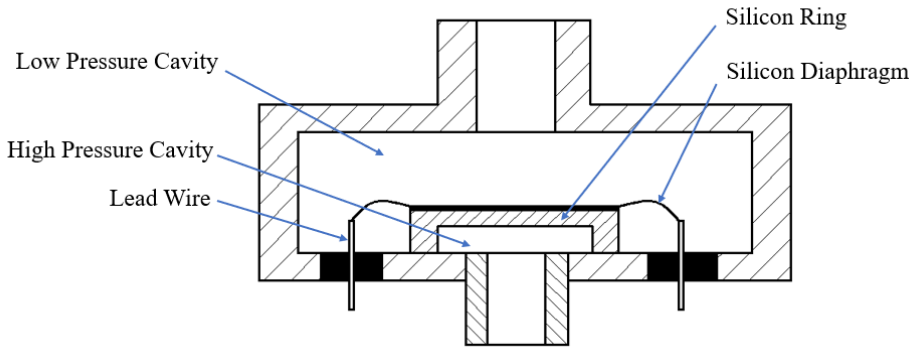

Fig.3-1 The structure of this high-temperature capacitive pressure sensor

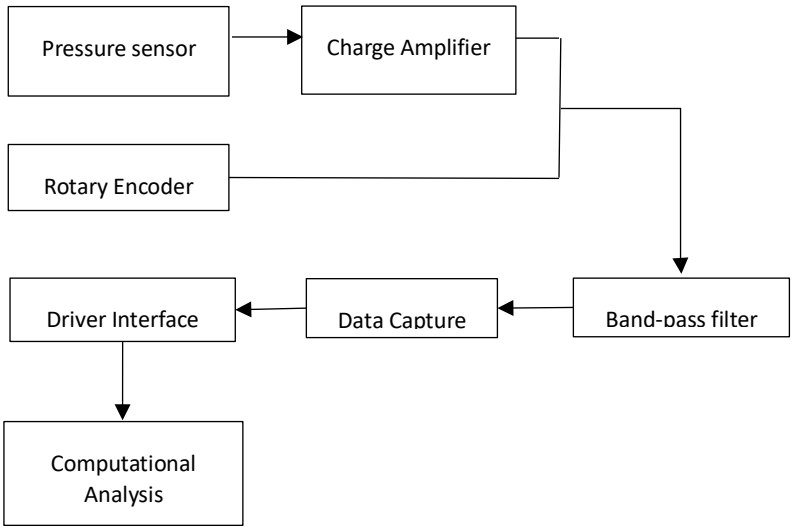

Figure 3-2: Knock excitation pressure measurement process

3.2 Knock Excitation Measurement

By applying mathematics integration, the in-cylinder pressure curve of the downsized engine during the knocking is obtained with respect to the time. The pressure curve of knocking shows the existence of abnormal combustion every three cycles, and hence, referred to as interval3. Fig. 3-3(a) indicates the variation of the in-cylinder pressure curves in terms of time.

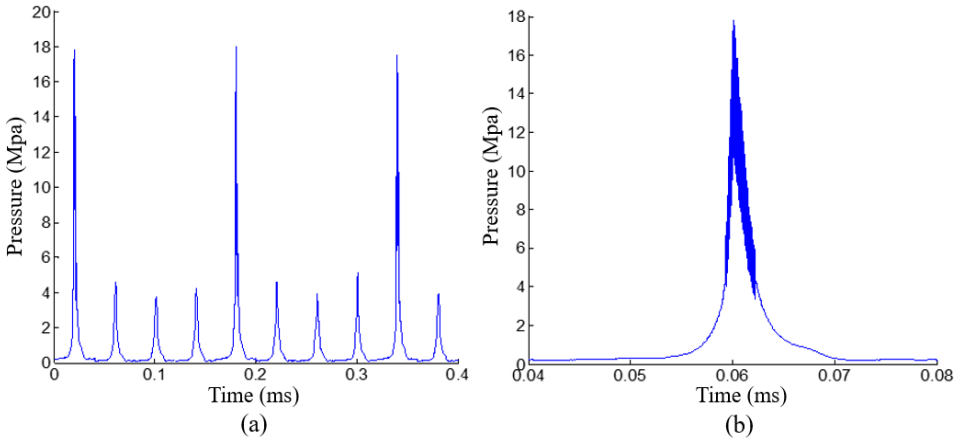

Fig.3-3 interval3 cylinder pressure and single-cycle cylinder pressure with the timing diagram

Fig. 3-3 (b) shows the single cycle curve of the knock and indicates that the maximum pressure reaches 18MPa when the knock occurs. Initially, a huge oscillation occurs with an amplitude of nearly 10 MPa, followed by a high-frequency oscillation with gradually reducing amplitude, and finally, the in-cylinder pressure is becoming steady. This phenomenon is the same as the numerical simulation as shown in Fig. 2-2 (b), and hence, the numerical simulation is validated.

4 Engine Knock Simulation

4.1 Finite element model of knock

The developed finite element model consists of two parts: the piston and the combustor flow field. Consider the meshing and actual calculation, the spark plugs, valves and certain chamfering are simplified. The remaining parts are modelled strictly according to the specifications, as shown in Table 4-1. Fig. 4-1 shows the developed 3D solid model.

Table 4-1 The piston specifications for the modelling

Parameters	Value
Piston outer diameter	74mm
Piston height	66.1mm
Pinhole diameter	15mm
Material	Grey cast iron
Poisson's ratio	0.3
Elastic modulus	125000MPa
Material density	7850kg/m3
Thermal expansion coefficient	1.1×10-5/℃

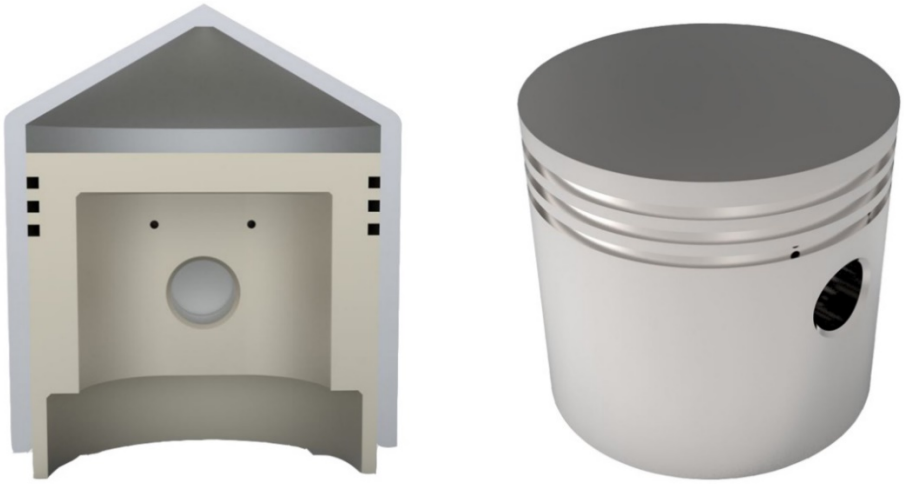

Fig. 4-1 3D solid model of the piston

Model meshing process is completed using the Meshing Platform. Starting with fluid region meshing, Physics Preference is chosen to be CFD; Relevance is set to 100, Relevance Center is set to Fine. The fluid region has then generated a mesh of 36,431 nodes, 197375 unit. The meshing process is then carried out for the solid region, $^1/_4$ of the entire piston model is used for the study as the solid region of the piston is a central symmetry structure. The Physics Preference is chosen to be Mechanical; Relevance is set to 100, Relevance Center is set to Fine. A refinement meshing is applied to the pin-hole and oil gap; Element size is set to 0.3 mm. The completed mesh is imported into the ICEM CED platform for the Quality inspection; the test results show that the Quality value is at least 0.2 which satisfy the application requirement. The upper part of Figure 4-2 is a mesh model of fluid and solid; the lower part is the mesh mass distribution of fluid and solid parts.

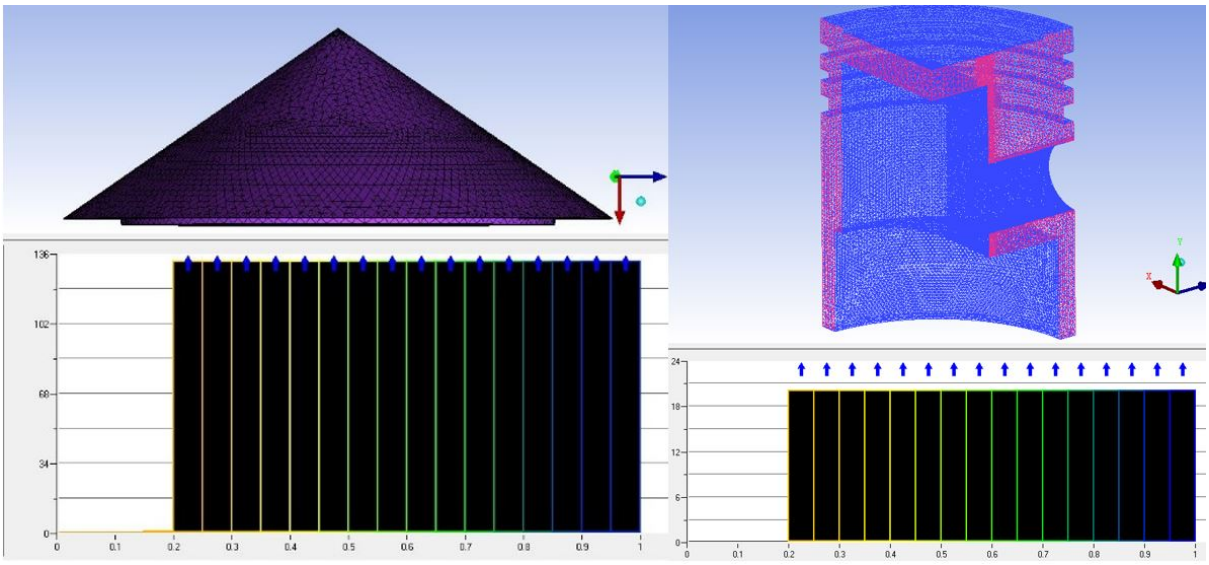

Fig.4-2 Finite element model of the cone-shaped combustion chamber

4.2 Initial conditions and solution model

According to the membrane breaking method which was proposed by Yao， the pressure oscillations have the most considerable fluctuation in the early stages of a strong knocking and cause the most damage to the piston. Therefore, this early stage pressure oscillation is simulated. Assuming the wall is insulated, the piston is at its stationary condition; the WALL boundary condition is set at the cylinder head and piston. The average in-cylinder pressure of 12 MPa is set at the end of compression stroke, based on the AFR of 28:1， a chosen value of 100 MPa for the high-pressure region of the naturally occurring point resulting in the formation of a required shockwave [13]. The 100 MPa high-pressure spherical area is placed at the centre of the model because placing it in other areas only affects the time when the shock wave reaches the shops of the piston cover without affecting the potential damage point position. The combustion chamber used in this simulation is considered to be a cone-top shape as shown in Fig. 4-3(a).Since the shockwave velocity is approximately 2000 m/s, the estimated time step is then calculated to be 8^{-10} seconds using $\Delta t = l/c$, where l, is the feature scales of the grid and c is the wave velocity. In addition, a Density-Based and Explicit solver is chosen and the third-order MUSCL is used as the

discrete format. This physical model adopts the ideal fluid model of K-epsilon (2eqn) turbulence flow. Regarding to the FLUENT, the model has become the primary tool in engineering flow field calculation since Launder and Spalding proposed it. This fluid model is a semi-empirical formula that is summed up from experimental phenomena and has a wide range of applications as well as been economical and reasonable accuracy. The model assumes that the flow is completely turbulent, and the influence of molecular viscosity is negligible. This is suitable for the flow of high Reynolds number, because the inertial force of the high Reynolds number flow is far greater than the viscous force, so that the viscous force can be neglected. Also, hence, suitable for fully turbulent flow process simulation. Prior to the simulating process, measurement points (named pm1 to pm8) are set from the centre of the piston to its outer edges in order to observing the overpressure distribution along this axis, as indicated in Fig. 4-3(b). The pressure curves of each of these locations are indicated by Fig. 4-5, as listed below.

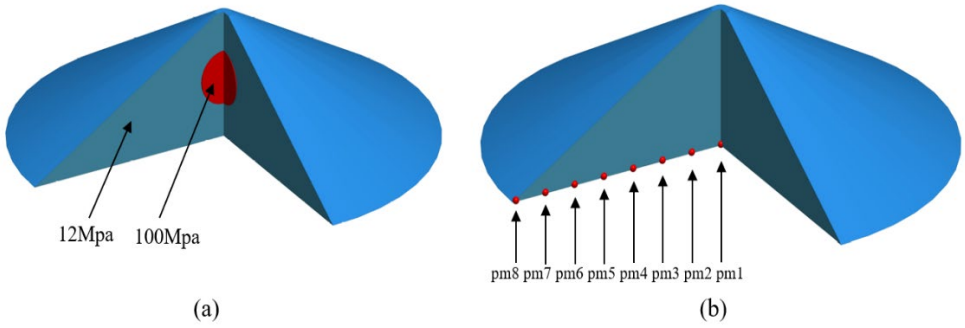

Fig.4-3 Cone-top combustion chamber model

4.3 Analysis of the knock simulation

According to the zero-dimensional simulation principle, the bottom surface of the combustion chamber corresponding to the top surface of the piston, and therefore, the 8-selected measurement points on the bottom of the combustion chamber correspond to the 8 locations on the top of the piston, as shown in Fig. 4-4.

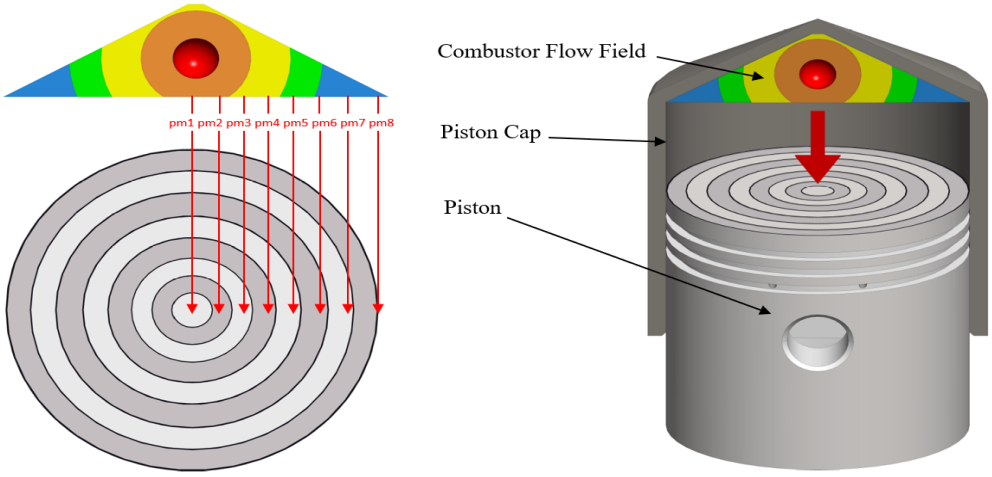

Fig.4-4: Setup of the measurement locations on the top of the piston

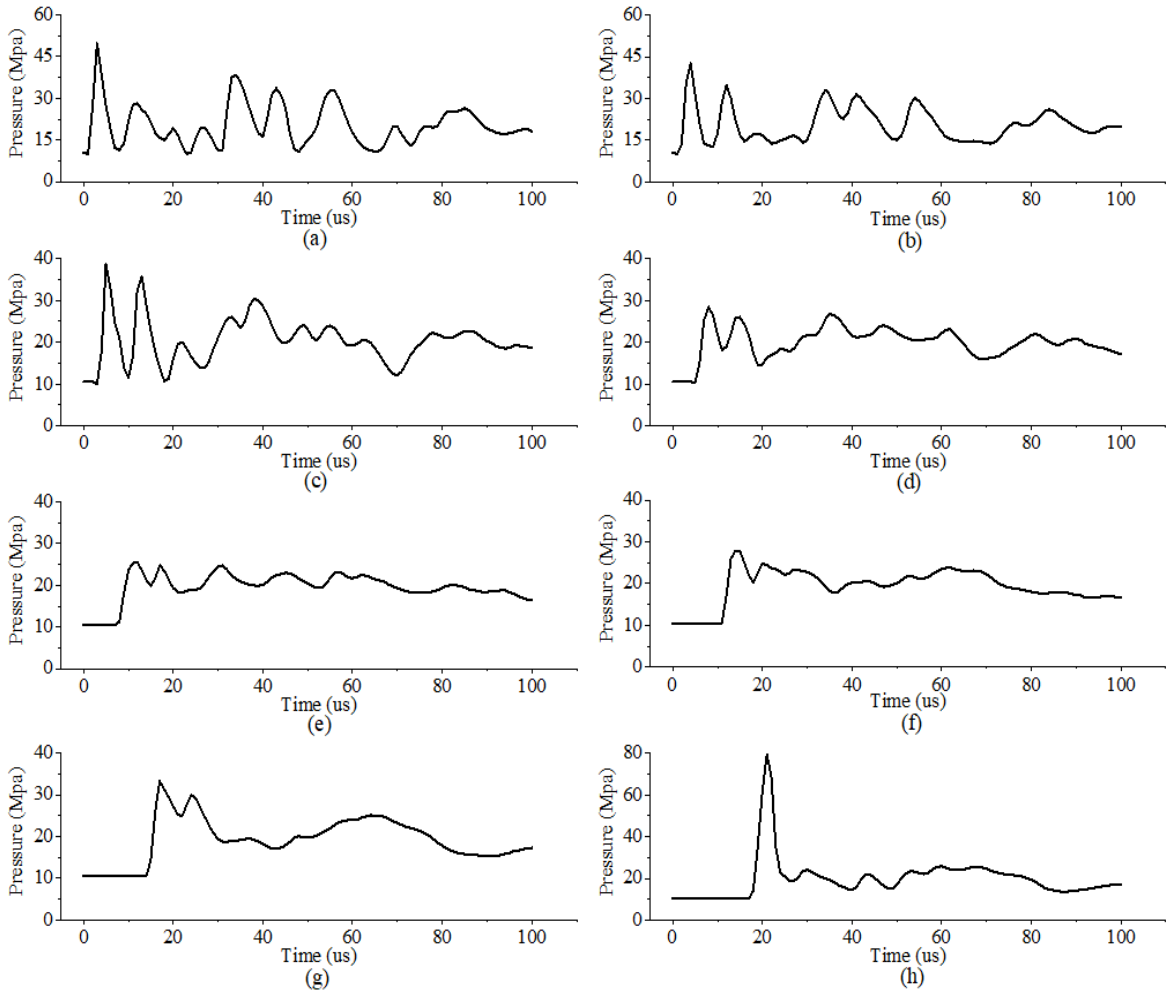

Fig.4-5 Pressure Fluctuation Curve at Position pm1 to pm8

Fig.4-5(a) shows a significant pressure oscillation with a maximum amplitude of 50 MPa occurs at the time of 5 us. Fig. 4-5(b) to Fig. 4-5 (g) indicates the maximum pressure at position pm2, pm3, pm4, pm5, pm6, pm7 is 42 MPa, 39 MPa, 29 MPa, 26 MPa, 28 MPa and 32 MPa, accordingly. In addition, these positions record 6 significant pressure oscillations with gradually decreasing amplitudes during the knocking period. Fig. 4-5(h) indicates the maximum pressure at position pm8 is 79 MPa and exceeding other points

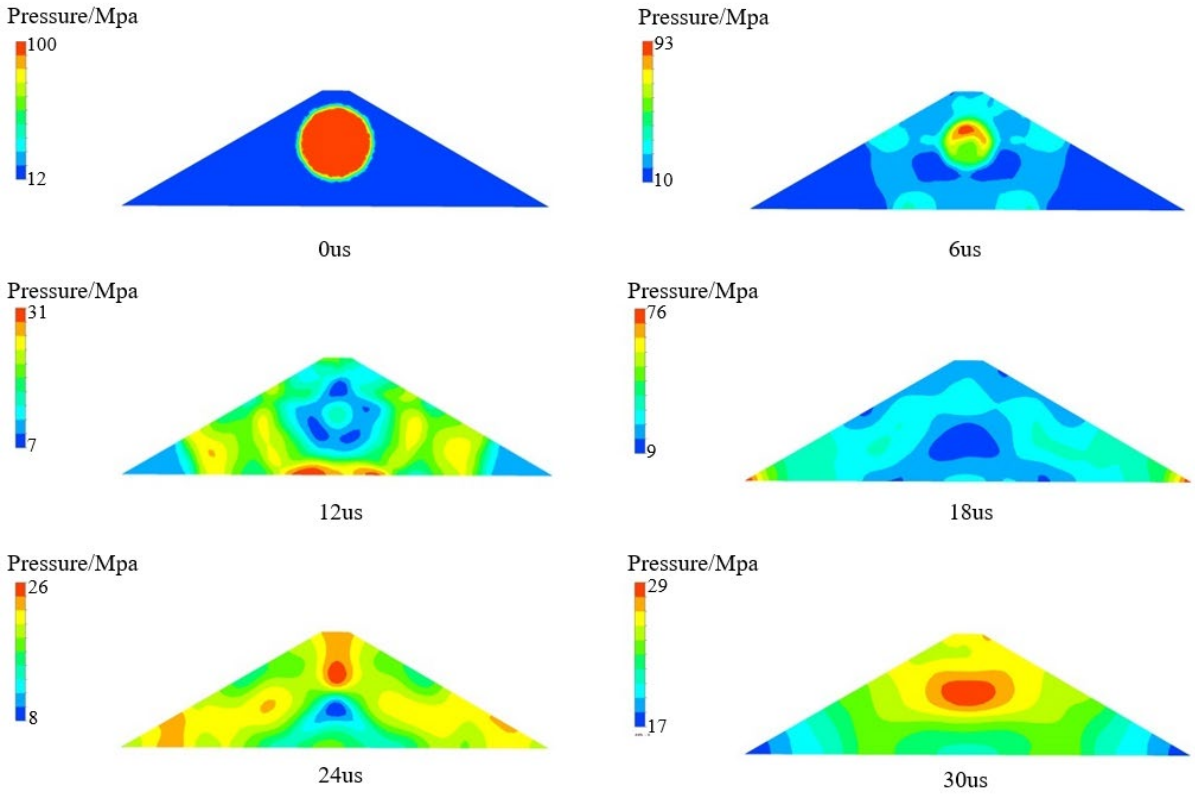

Fig.4-6 Numerical simulation results of combustion chamber flow field

Fig. 4-6 indicates that the cross-section pressure distribution map of a combustion chamber numerically simulated. It shows the high-pressure zone from 0 to 20us is in the diffusion stage, and the shock wave extends from the centre to the edge. The shock wave then begins to reflect, including up and down reflections (between the cylinder head and the piston) and between the centre and edge of the combustion zone.

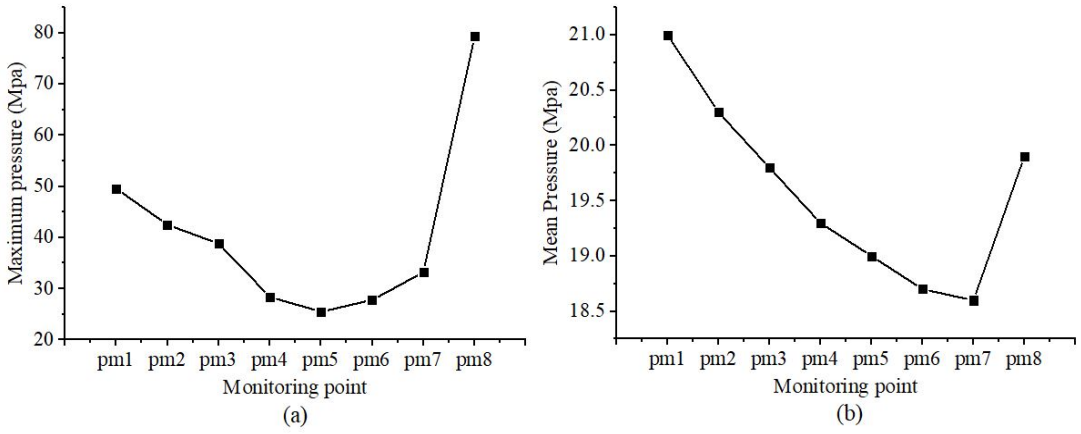

Fig.4-7 Maximum pressure and Mean pressure at various measurement positions

Figure 4-7 (a) indicates that the maximum pressure chart of eight monitoring points. The maximum pressure of pm8 at the edge position is much higher than that at

other monitoring points. This is because the number of shockwave reflections between the cylinder head and the piston increases exponentially as the gap between the cylinder head and the piston decreases when the shock wave reaches a narrow area at both ends. When the edge position is compressed by geometric shape, the pressure rises rapidly. Fig. 4-7 (b) indicates that the mean pressure chart of 8 monitoring points. According to the figure, the monitoring point pm1 in the centre position has the highest mean pressure, and the mean pressure decreases gradually as it approaches the edge, while the monitoring point pm8 in the edge position has higher average stress than several nearby monitoring points, but lower than the monitoring point pm1 in the center position. To conclude, the results indicate that the piston centre and edge are predicted to experience failure firstly due to the tremendous pressure values.

5 Knocking strength calibration

5.1 Boundary conditions of the piston thermal-mechanical coupling

The piston is mainly subjected to thermal load and mechanical load during the engine operation. The thermal load acts on the entire piston and leads to differences in the temperature gradients at various locations of the piston. Therefore, the thermal expansion at each of these locations are different and resulting in differences in the extent of deformation and stress-strain. The mechanical load mainly consists of the in-cylinder gas explosive pressure, reciprocating inertia, side thrust and friction forces and so on. The explosive gas pressure plays a significant role regarding the mechanical load, whereas, the reciprocating inertia and friction are relatively small and therefore, is neglected. The slide thrust is affected by various factors and is very complex to solve. Therefore, only the mechanical load due to explosive gas pressure is considered in this paper. In addition, the thermal load and mechanical load are coupled with each other. Hence, thermal-mechanical coupling modules are applied.

The temperature field of the piston basically remains unchanged while the engine is operating steadily. The third-type of thermal boundary conditions with the convective heat transfer coefficient is applied to calculate the piston temperature field. The required convective heat transfer coefficient and an average temperature of the media is determined by empirical formula and literature. This paper focuses on the most destructive reflections occurs at the initial stage of the knock, the piston velocity is relatively slow near the top dead centre during this stage, and therefore, the piston motion is considered to be at resting. In order to apply this consideration to the model, a normal constraint is applied to the piston pinhole to limit the axial movement and leave the remaining directions free of movement.

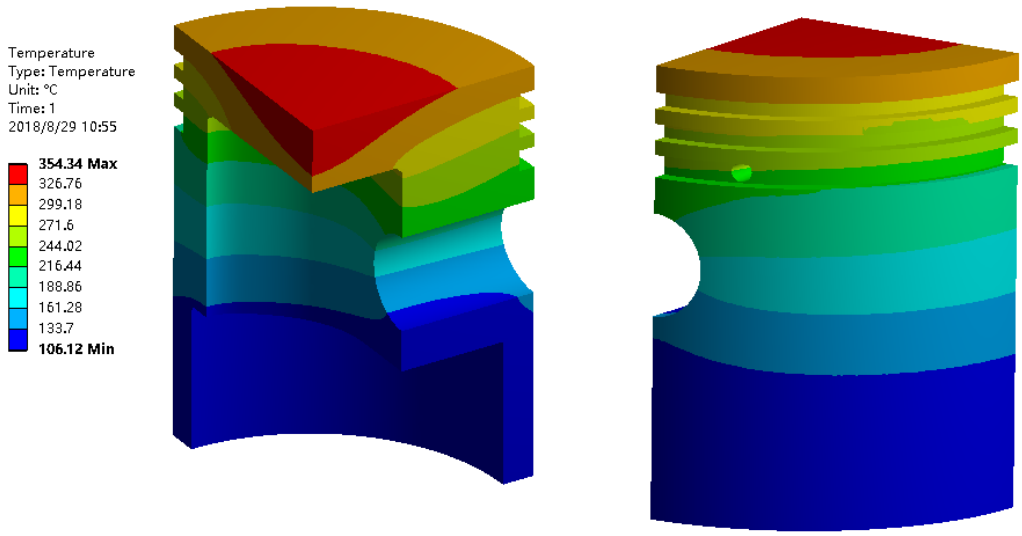

Fig.5-1 Piston temperature profile

Fig. 5-1 indicates a non-uniform temperature distribution on the piston top surface. The temperature is gradually decreasing from the center of the surface to the edge with a maximum value of 354 ˚ C. The remaining part of the piston, including the piston cavity, has the temperature of 106 ˚ C, and therefore, a temperature difference of 248 ˚ C is formed, which matches with the actual condition. Also, the piston model material is set as grey cast iron which has a maximum temperature range of 700 ˚ C to 950 ˚ C, and therefore, the entire temperature field is within this range to prevent the phenomenon of the burning top. When the engine is stable, the internal temperature of the engine is also stable under the action of the engine cooling system. Therefore, the initial conditions of the subsequent simulation are set to 350 °C.

5.2 Piston top strength analysis

Based on the thermal-mechanical coupling boundary conditions, the results from numerical simulation and simulation of the cylinder pressure excitation curve are applied to determining the stress field and deformation field of the piston top surface under different conditions. Because the stress field and deformation field of the piston top surface is not constant. Therefore, as shown in Fig. 5-2, the maximum stress values and the maximum deformation values of the 8 monitoring points on the top surface of the piston are sorted out.

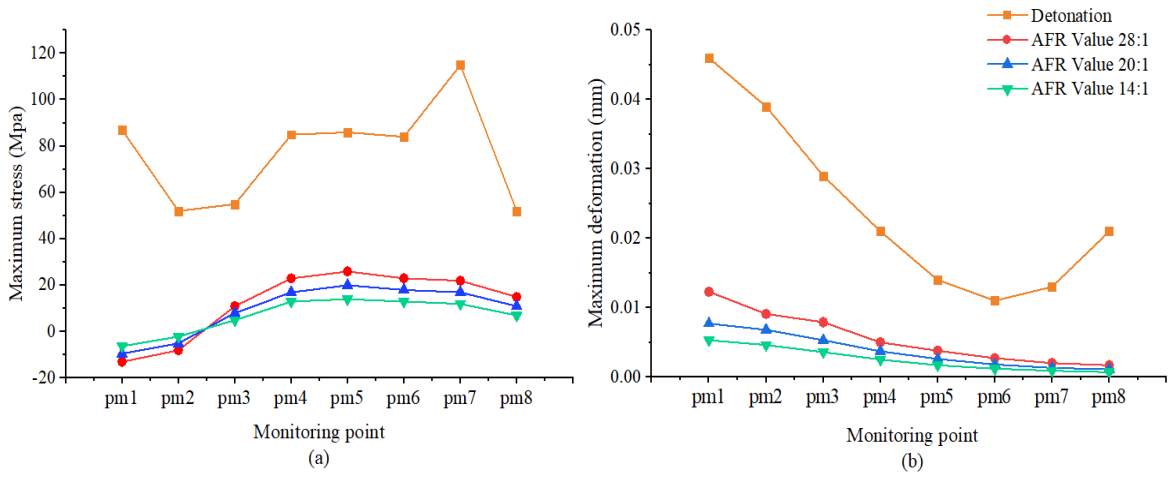

Fig.5-2 Stress deformation values for different operating conditions at different positions on the top of the piston

Fig. 5-2 (a) indicates that the maximum stress diagram of each monitoring point on the top of the piston. The stress value decreases gradually from the center of the top of the piston to the outer edge and then increases gradually. The stress values of all measured positions increase with the increase of pressure intensity. The stress value in the detonation process is obviously greater than other conditions. Fig. 5-2 (b) indicates that the maximum deformation of each monitoring point on the top of the piston, and the same trend is used in natural suction and boosting. They all gradually become stable. The figure also shows that the deformation value increases with the increase of pressure, and the maximum deformation occurs during the detonation event, and the curve performance is different. During the detonation process, the deformation value decreases slightly in the early stage and then increases to the maximum. This is because the pressure is not uniformly distributed during the tapping on the top surface of the piston. The maximum pressure exists at the edge of the piston and decreases toward the centre, as shown in Figure 4-7.

5.3 Piston strength analysis and calibration

The occurrence of engine knock not only affects the stress and deformation of the top surface of the piston but also the remaining part of the piston. Fig. 5-3 indicates the stress and deformation of the entire piston under various AFR cases. The stress curves have the same trend as the in-cylinder pressure curves. The maximum stress and deformation occur at the point of maximum in-cylinder pressure, and they are increasing with an increase in the pressure intensity.

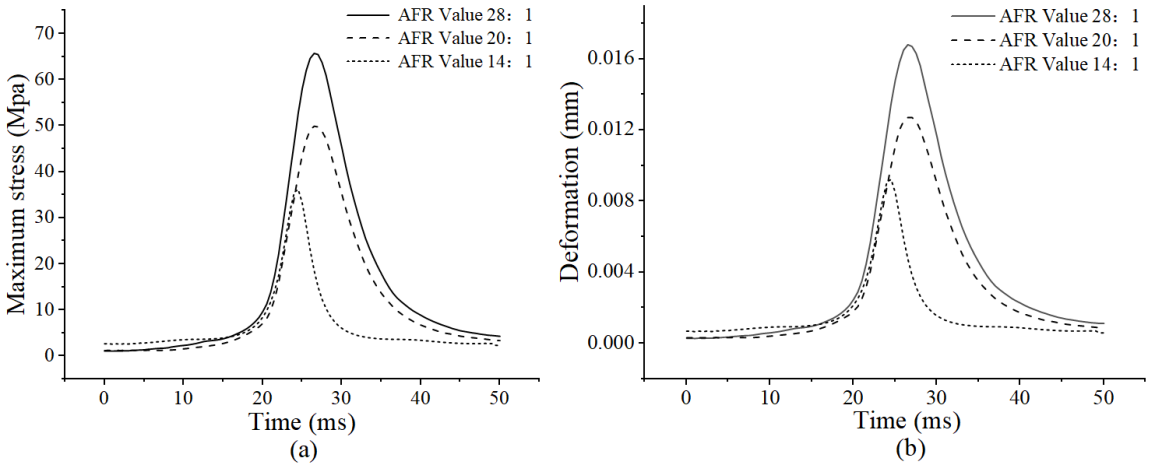

Fig.5-3 Deformation and stress curves of pistons under different working conditions

Fig. 5-4 to 5-6 shows the maximum principal stress and total deformation of the whole piston under various working conditions. While AFR is 14:1, the maximum principal stress (tensile stress) is about 26.7 MPa, the minimum principal stress (compressive stress) is about 9 MPa, and the maximum deformation is 0.008 mm. While AFR is 20:1, the maximum principal stress (tensile stress) is about 49.9 MPa, the minimum principal stress (compressive stress) is about 16.9 MPa and the maximum deformation is 0.012 mm. While AFR is 28:1, the maximum principal stress (tensile stress) is about 65.7 MPa, the minimum principal stress (compressive stress) is about 22.2 MPa and the maximum deformation is 0.016 mm. Under all three conditions, the maximum stress is concentrated on the piston pin hole. Secondly, due to the direct pressure exerted on the centre of the piston top, the stress at the centre of the piston chamber is larger. The maximum compressive stress in all three cases occurs at the junction of the piston cavity and the piston head because the downward movement of the piston head centre compresses the internal junction and produces a stress concentration area around the junction. According to the first strength theory, the maximum principal stress in all cases is less than the strength limit of grey iron, that is 280 MPa, to meet the strength requirements. In addition, under all three conditions, the maximum deformation occurs at the bottom of the piston body. This is because the bottom of the piston body is a weak area of the piston, and the stiffness is relatively small, so it is easier to deform. For all three cases, due to the constraint and support of the piston pin, the deformation near the top pin hole of the piston is minimal, so the deformation in this area is small. As a result, the deformation value at the centre of the piston head is larger and gradually decreases towards the outer edge. The deformation value does not exceed the standard tolerance 0.2mm between the piston and the cylinder wall to meet the requirements.

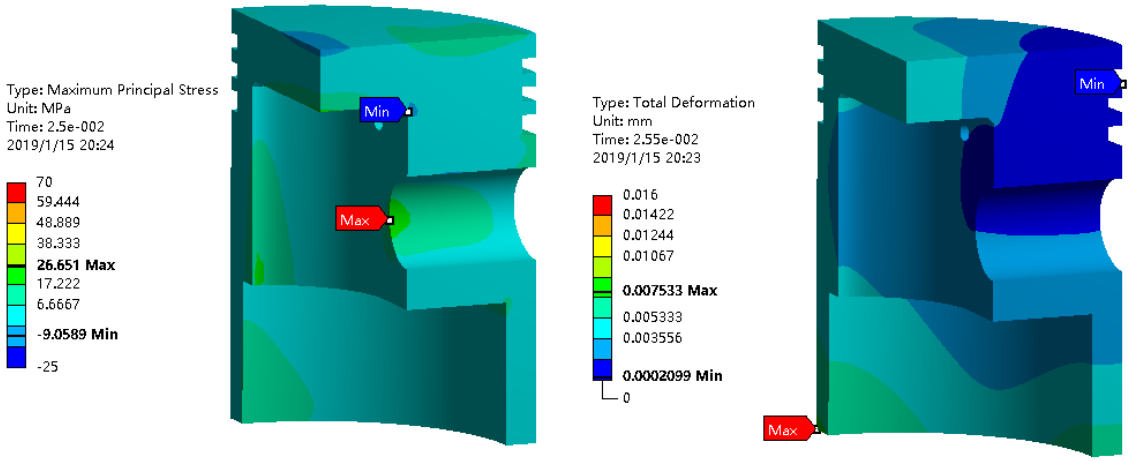

Fig.5-4 Stress and deformation distribution of the piston with AFR of 14:1

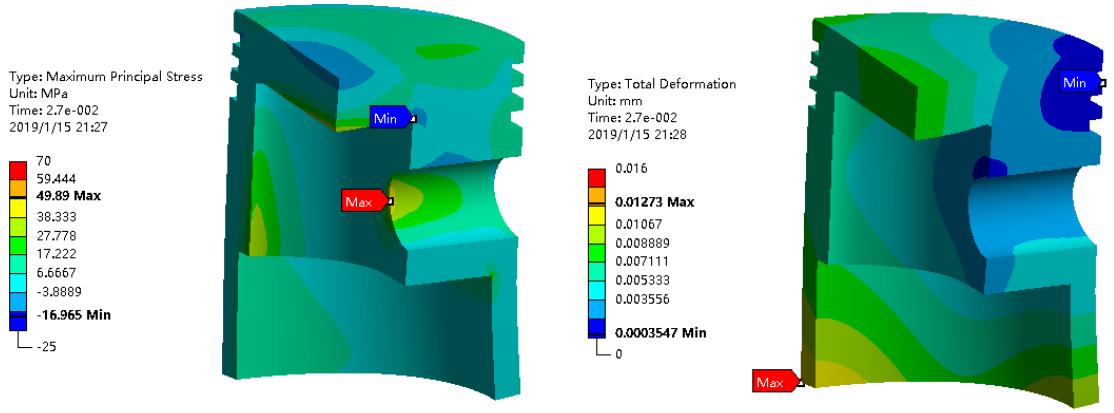

Fig.5-5 Stress and deformation distribution of the piston with AFR of 20:1

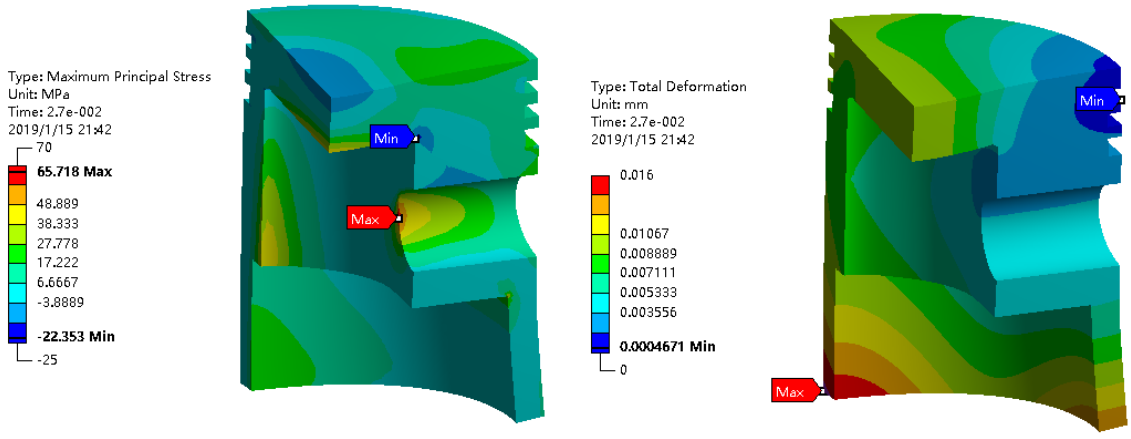

Fig.5-6 Stress and deformation distribution of the piston with AFR of 28:1

The pressure fluctuation curve on the piston surface is obtained by solving the flow field part. The monitoring points are distributed from the bottom of the combustion chamber, i.e. the centre of the top surface of the piston to the edge of the piston, eight circles are formed by taking the distance between the measuring points and the centre of the top surface of the piston as the circle centre. The stress-strain and deformation distribution of piston under detonation are calculated. The schematic diagram of loading is shown in Figure 5-7.

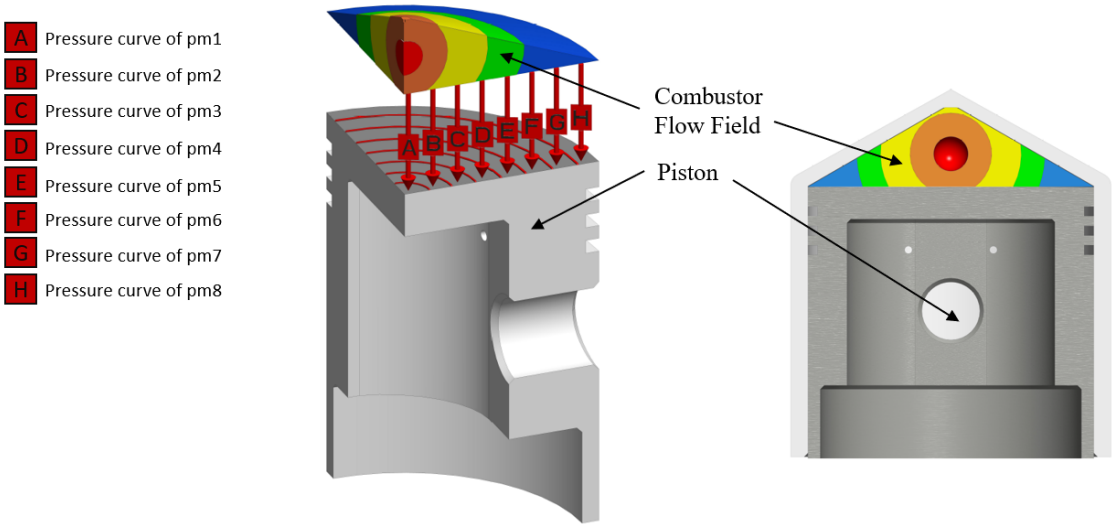

Fig.5-7 Schematic diagram of pressure on piston top surface

Fig. 5-8 indicates the maximum stress and deformation of the whole piston in time of detonation change with time. It shows the stress and deformation curves in the piston knock state are higher than those in the non-detonation state. As can be seen from the diagram, the stress and deformation show a gradual increase and stable trend, and the stress in the process of increasing vibration. The reason is that the pressure distribution in the combustion chamber is very uneven because of the multiple reflections of the shock wave in the combustion chamber at the initial stage of detonation. With the fusion of high- and low-pressure regions, the pressure in each position of the combustion chamber is gradually stabilized, and the stress and deformation of the piston are also stable.

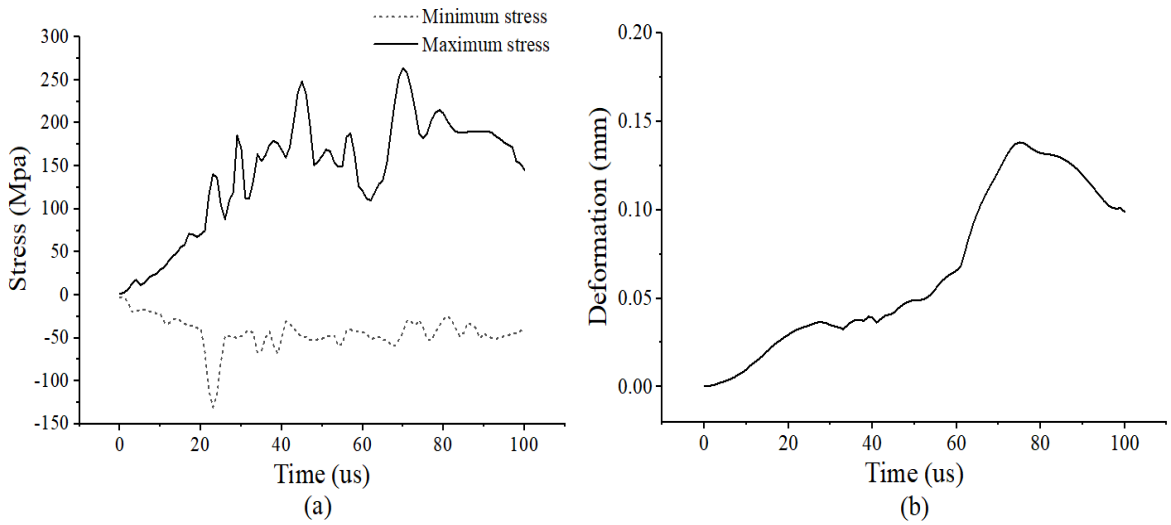

Fig.5-8 Deformation and stress curve of the piston during the knocking

Fig. 5-9 shows the maximum principal stress and maximum deformation during the detonation process. The maximum tensile stress is about 252 MPa and appears on the surface of the piston cavity. The maximum compressive stress is about 52 MPa, which appears on the outer surface of the piston. The maximum principal stress is less than 280 MPa of grey cast iron, so as to meet the requirements. The maximum deformation under detonation is 0.138 mm at the bottom of the piston body. The deformation of the top of the piston increases from top to bottom. The results show that the standard tolerances with coupling deformation less than 0.2 mm meet the requirements.

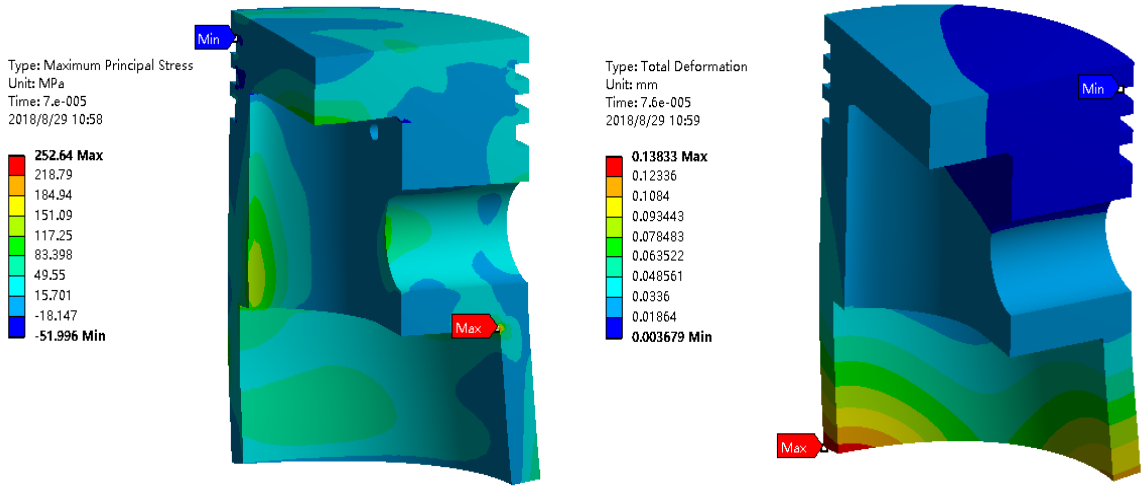

Fig.5-9 Stress and deformation distribution of the piston during the knocking

In summary, the occurrence of the engine knock increases the stress and deformation at each measurement location and the inner cavity. Also, the position of the maximum stress and maximum deformation is changed during the knocking, in other word, the potential failure point is changed. However, the simulation results from the developed piston model show that the piston toughness is still within its

strength limit and the deformation does not exceed the standard tolerance. Therefore, the piston is still satisfying the requirement under the knock condition.

6 Simulation and analysis of the piston fatigue under the knock

6.1 The theory of the piston fatigue under the knock

During the occurrence of the engine knock, a strong detonation wave is generated in the combustion chamber, and this wave is a type of the shockwaves; This shockwave applies a repeated high-frequency impact load on the piston. When the piston receives this shockwave multiple time, the crack is created and developed into a fracture rupture due to accumulative damage. This is the basic process of the piston failure introduced by the shockwave. During this process, the stress and strain created by this impact load are known as the impact of stress and impact strain [14].

The damage category regarding each specific component is identified according to the working environment and conditions of the specific component while the characteristics of the repeated load are fully considered. Then, the fatigue life of the piston under the effects of the knock wave is determined by applying the corresponding fatigue damage theory based on the identified category. T. H. Ren. (2014) has derived the equations for the study of the damage caused by the impact of fatigue [15] and is shown as the following:

$$\delta D = \int_t \ \Omega \ dt \qquad \text{(Eq. 6-1)}$$

where Ω is the damage variable under single load; D is the impact fatigue variable corresponding the number of cycles. Due to the fact that material damage is anisotropic, the impact fatigue damage variable increment can be written as:

$$\delta D_i = \int_t \ \frac{\delta \Omega_i}{\delta t} \ dt \qquad \text{(Eq. 6-2)}$$

where, Ω_i is the damage variable in the i^{th} direction under a single load; Di is the impact fatigue variable in the i^{th} direction corresponding the number of cycles;

Considering the cumulative damage caused by a single impact load is the integral of the damage evolution rate $\dot{\Omega}$ with respect to the time t, hence, the impact fatigue damage caused by the single impact load is calculated by the following equation:

$$\frac{\delta D_i}{\delta N} = \int_t \ \dot{\Omega}_i \ dt = \int_t \ \delta \Omega \qquad \text{(Eq. 6-3)}$$

While $N = N_0$ (the number of load cycles required to cause the occurrence of the fatigue crack initiation, also known as the number of load cycles before the damage occur), D = 0, and thus the impact fatigue equation can be expressed as:

$$D_i = \int_{N_0}^{N} \frac{\delta D_i}{\delta N}\, dN = \int_{N_0}^{N} A\ dN \qquad \text{(Eq. 6-3)}$$

6.2 Fatigue modelling and analysis of the simulation results

Fig. 6-1 shows a systematic block diagram to indicate the fatigue analysis strategy.

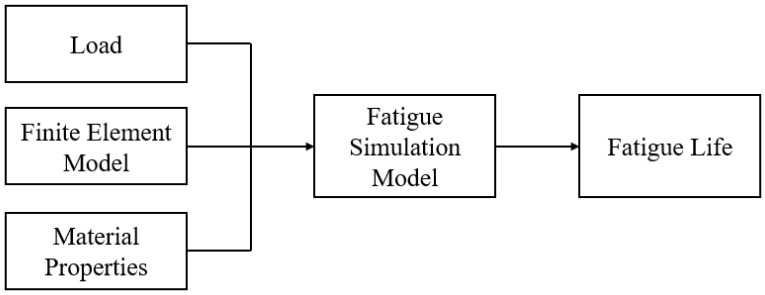

Fig.6-1 Systematic block diagram of the fatigue analysis strategy

The method of fatigue simulation analysis is listed as the following:

Finite Element model: The developed previous finite element model is imported into the fatigue simulation model. This FE model includes the strength calibration results and stress and strain results. The potential failure point can be determined by analyzing the finite element model.

Material Fatigue Characteristics: The simulation software used is called, Ansys-workbench. Its database contains the corresponding properties and S-N curve of the piston material, grey cast iron, that is required to proceed with the fatigue simulation.

Load spectrum: The pressure-time history of the component structure is obtained by going through the flow field analysis, and then, this pressure-time history is multiplied by the stress results from the strength calibration section to provide the stress-time history that required by the fatigue analysis. The rain-flow counting method is used to count the load spectrum.

Fatigue Analysis Model: This model includes the fatigue life analysis method, stress combination method and stress correction method. The fatigue life prediction method used in this paper is the nominal stress method, the stress combination method is chosen to be SignedVonMises, and the stress correction method is chosen to be Doodman.

Finally, the Fatigue simulation and analysis: Determining the number of load cycles by giving the service life. Then the safety factor of all parts of the piston under this cycle is solved. Judging whether the piston meets the life requirement through the safety factor. And get the piston's dangerous position.

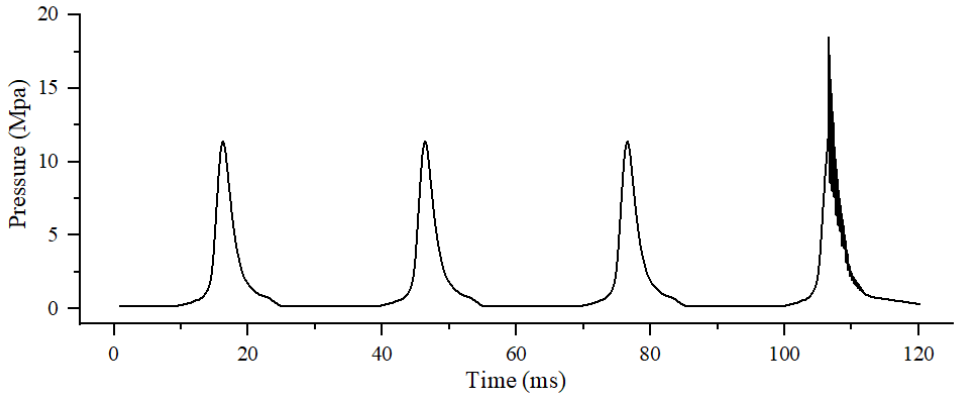

Fig.6-2 Load spectrum of fatigue analysis

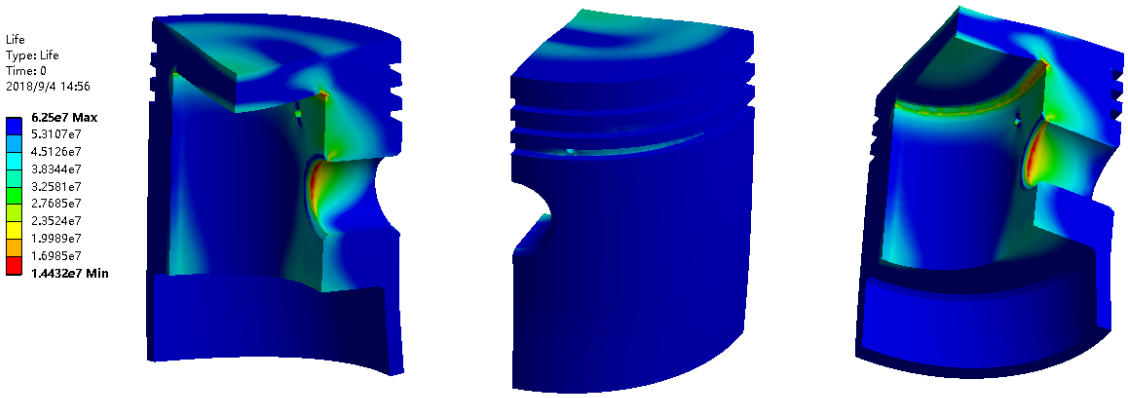

Fig.6-3 visualization diagram for the fatigue life

In normal conditions, knock occurs every 3 or 4 normal cycles. Fig. 6-2 indicates Load spectrum for this life analysis and think that knock occurs every 3 normal cycles. The piston cyclic life is determined by applying the load spectrum to the piston top surface, and the results are presented in Fig. 6-3. Considering the engine is operating at 100 km/h, all three fatigue life diagrams indicate the number of cycles is at least 1.44 x 107. The calculated continuous mileage of the engine is 253,440 km, which exceeds the requirement of 220,000 km. At the same time, it is possible to predict the initial damage occurring on the surface of the piston pin hole and the joint of the piston cavity.

7 Conclusion

In this paper, a numerical simulation is developed to obtain the in-cylinder pressure curves of the gasoline engine under various operating conditions and the knock conditions; The results of the numerical simulation are validated against the knock excitation experiment, and hence, the pressure fluctuation characteristics of the engine knock are determined.

Also, based on Rover K16 gasoline engine, the engine knock phenomena inside the combustion chamber is simulated using the Fluent simulation method. The

pressure fluctuation pattern on the bottom of the combustion chamber also referred to as the top surface of the piston, is obtained by measure the characteristics at the selected locations. The results show that the maximum pressure occurs at the edge of the piston top surface.

Furthermore, using the ANSYS simulation method, the influence pattern of the piston stress and deformation under the knock is obtained by comparing the stress and deformation of the piston under various working conditions. The piston strength and deformation degree are judged based on the first strength theory and the standard tolerance of the gap between the piston and the cylinder inner wall.

Finally, the fatigue simulation method is used to predict the initial damage of piston in the process of detonation at the surface of the piston pin hole and the joint of piston cavity. The calculated continuous mileage of the engine is 253,440 km, which exceeds the requirement of 220,000 km.

Reference

[1] Wang Z, Long Y, and Wang JX. Advances in premature combustion and super detonation of turbocharged gasoline engines. *Journal of Automobile Safety and Energy Conservation,* 2015,6(01): 17-29.

[2] Zahdeh A, Rothenberger P, Nguyen W, et al. Fundamental Approach to Investigate Pre-Ignition in Boosted SI Engines. *SAE International Journal of Engines,* 2011.

[3] Haenel P, Seyfried P, Kleeberg H, et al. Systematic approach to analyze and characterize pre-ignition events in turbocharged direct-injected gasoline engines. S*AE Tech Paper,* 2011-01-0343.

[4] Peters N, Kerschgens B and Paczko G. Super-knock prediction using a refined theory of turbulence. *SAE International Journal of Engines*, 2013

[5] Qi YL, Xu YQ and Wang Z. Knock characteristics of gasoline engine induced by simulated early combustion. *Journal of Engineering Thermophysics,* 2014,35 (06): 1227-1231.

[6] Luo X, Teng H, Hu T, et al. Mitigating intensities of super knocks encountered in highly boosted gasoline direct injection engines. *SAE Paper*, 2015-01-0084 , 2015.

[7] Wang Z, Shuai JS and Wang JX. Numerical simulation of knock combustion process for spark ignition engines. *Journal of Engineering Thermophysics,* 2013,34 (04): 775-778.

[8] Lv M and Bao XF. Super detonation test and Simulation of TGDI gasoline engine based on double injection. *Journal of Internal Combustion Engines,* 2016,34(06): 518-523.

[9] Wang Z, Qi YL ,Liu H, et al.Experimental study on pre-ignition and super-knock in gasoline engine combustion with carbon particle at elevated temperatures and pressures. *SAE Tech Paper*,2015 -01-0752 .

[10] Manfred A, Terrence A, Darius M. The Effect of EGR on Low-Speed Pre-Ignition in Boosted SI Engines. *SAE International Journal of Engines*, 2011, 4(1):235-245.

[11] Winklhofer E, Hirsch A, Kapus P, et al. TC GDI engines at very high power density-irregular combustion and thermal risk. *SAE Paper 2009-24-0056.*

[12] Zaccardi J, Duval L and Pagot A. Development of Specific Tools for Analysis and Quantification of Pre-ignition in a Boosted SI Engine. *SAE 2009-01-1795.*

[13] Yao CD and Xu H. The piston failure mechanism of cone shock chamber for cone top combustion chamber. *Explosion and Impact*, 2015, 35 (1): 57-64.

[14] Tian C. Thermal-mechanical coupling analysis and fatigue life prediction of the piston of the YC6MK375N CNG engine. *Wuhan University of Technology*, 2013, in Chinese.

[15] Ren TH, Zhang WH and Xue XH. Study on the fatigue damage properties of foundation soil under impact loading. *Journal of hydraulic engineering,* 45 (5), 2014.